

CMOS-Compatible Thermally Actuated MEMS Viscosity Sensor with Aluminum on Silicon Plate

Ivan Puchades, Lynn F. Fuller and Sergey Edward Lyshevski

Department of Electrical and Microelectronic Engineering, Rochester Institute of Technology
Rochester, NY 14623

E-mail: ixpeme@mail.rit.edu; lffeee@rit.edu; seleee@rit.edu

ABSTRACT

In the fields of rheology and tribology, viscosity is one of the most important factors used to characterize fluid properties. In the automotive, aerospace, energy, naval, transportation and other applications, oil is used as an engine and motion devices lubricant. It is imperative that the oil viscosity is kept within a specific range to provide the needed functionality, safety, high performance, etc. The higher the viscosity, the more resistance the liquid creates and the harder to operate for machines. These lead to low efficiency, temperature increase, low fuel economy, damages, etc. If the viscosity is too low, oil will not provide sufficient protection leading to wearing and unsafety.

Keywords: CMOS; MEMS; sensors; viscosity

1. INTRODUCTION

MEMS devices provide an opportunity to measure the fluid viscosity. Current MEMS-based viscosity sensors utilize changes in resonant frequencies of cantilever beams, plates, membranes or quartz crystals to detect and measure the viscosity which varies. In these vibration viscometers, the damping of an oscillating electromechanical resonator, which is immersed in the test liquid, is measured. Complex actuation and sensing methods, which are usually non-CMOS compatible, make these devices expensive. Furthermore, fabrication and integration is very difficult. References [1-3] use an electromagnetic driven cantilever beam or plate. This requires the use of a strong external magnet and an optical readout which cannot be integrated within low-cost CMOS platforms. Reference [4] uses ZnO to achieve ultrasonic piezoelectric actuation of a long microprobe with a piezoresistor read out. However, ZnO is not a standard CMOS material, and, the length of the vibrating microprobe raises structure reliability questions. Reference [5] proposes the use of ZnO as a piezoelectric membrane. Piezoelectric quartz crystal and ZnO are studied in [6] and [7] to correlate changes in the transmitted surface acoustic wave frequency to density and viscosity changes.

Our solution solves the CMOS compatibility problem and avoids the use of external components for actuation and read out. It is based on thermally induced vibrations of a silicon plate and its damping due to the surrounding fluid. This vibration viscometer device utilizes thermal actuation through an in-situ resistive heater and piezoresistive sensing,

both of which utilize CMOS compatible materials. This leads to affordable and reliable systems. A technology-centric solution is verified, tested and characterized.

2. THEORETICAL FOUNDATIONS

When a supported thin plate, shown in Figure 1, is rapidly heated, it deflects because it expands due to heat. A static deflection is due to the temperature increase. Dynamically, the response corresponds to an under-damped system. The dynamics of the plate displacement from an initial to final position is studied. There are well-defined equilibriums. The thermal vibration frequency is independent of the pulse heat or temperature, and, it corresponds to the natural frequency of vibration of a supported square thin plate. The frequency can be calculated using the following equation [8]

$$f = \frac{19.74}{2\pi a^2} \sqrt{\frac{Eh^3}{12\rho h(1-\nu^2)}}, \quad (1)$$

where E is the Young's modulus of the material; a is the length of plate; h is the thickness; ρ is the density; ν is the Poisson ratio.

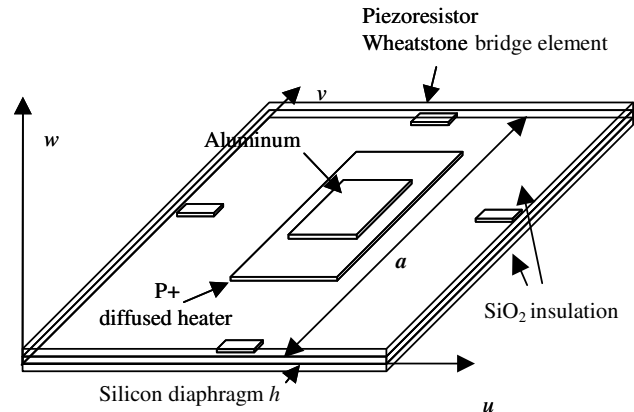


Figure 1. Graphical representation of the thin silicon diaphragm with the p+ diffused heater actuator, the aluminum bimetal area, and piezoresistor Wheatstone bridge sensing elements

This analysis is valid if the structure is rapidly heated. The thermal properties of the system affect the amplitude of the vibration, and, have no effect on the frequency of oscillation. The rate of heating has to be faster than the characteristic thermal time t_0 of the structure which is defined as $t_0 = h^2/\kappa$. For a silicon diaphragm with $h=15 \mu\text{m}$, $t_0=2.8 \mu\text{s}$.

We use pulse heating rather than a step heat input to prevent heating of the fluid.

The relation of the natural angular frequency of the plate vibrating in vacuum ω_{vacuum} and in fluid ω_{fluid} depends on the density of the fluid ρ_{fluid} , plate material ρ_{plate} , radius a and thickness h of the circular plate. According to [9]

$$\omega_{fluid} = \frac{\omega_{vacuum}}{\sqrt{1+\beta}}, \quad \beta = 0.669 \frac{\rho_{fluid} a}{\rho_{plate} h}, \quad (2)$$

where β is the virtual mass.

The viscous effect on frequency is found to be negligible for macroscopic plates. This assumption cannot be used when the thickness of the plate is within micrometers. The analysis of the micromachined piezoelectric circular membranes vibration in liquid is researched in [5]. The model [9] matches well for dynamic viscosities of less than 10 centipoise (cP). The viscosity of water at room temperature is 1 cP= 1×10^{-3} Pa.s. Beyond the 10 cP value, the shift in the natural frequency is larger than that predicted in [9]. It is also reported that the Q value of the resonance degrades as the viscosity increases and more rapidly as the viscosity is greater than 10 cP [9].

The revised analysis [10] uses the viscosity of the liquid as an energy dissipative element. The viscosity of the fluid actually couples the plate vibration to the tangential velocity of the fluid, thus increasing the fluid movement and its kinetic energy. The modified virtual mass factor is

$$\beta = 0.6538 \frac{\rho_{fluid} a}{\rho_{plate} h} (1 + 1.082\xi). \quad (3)$$

The energy dissipation of the system is characterized by ξ . This ξ depends on the kinematic viscosity ν which is defined as the ratio of dynamic viscosity η and density ρ , radial frequency of vibration ω , and the membrane radius a . In particular,

$$\xi = \sqrt{\nu / \omega a^2}. \quad (4)$$

The quality factor Q is defined as the ratio between the energy stored E_{stored} and energy dissipated $E_{dissipated}$ per cycle. We have

$$Q = 2\pi E_{stored} / E_{dissipated} \approx 0.95 / \xi. \quad (5)$$

Knowing the resonance frequency and the quality factor in the liquid, we can calculate the density and the viscosity of the liquid.

3. MICROFABRICATION

A bulk MEMS microfabrication process is used to fabricate the actuator/sensor structure. Silicon was used as the bulk and heater material, while, SiO₂ is an insulating layer, and, polysilicon is strain gages for sensing the vertical displacement. The interconnect and bimetallic effect are achieved using Al. The bimetallic effect is due to the difference in thermal expansion coefficient of the silicon diaphragm and the aluminum layer deposited on top of it. This bimetallic effect is used to enhance the bowing effect of the silicon diaphragm. A diaphragm width and length of 2.5 mm and thickness $h=15 \mu\text{m}$ is chosen for maximum vertical

displacement while maintain a linear behavior [9, 10].

The fabrication process starts with double-side-polished n-type silicon on oxide (SOI) wafers. The top silicon layer is 15 μm thick and the buried oxide is 1 μm thick. A silicon oxide is grown and used as a masking layer for the p+ spin-on-dopant process, which acts as the heating element of the membrane. After this, a pad silicon oxide is thermally grown. Silicon nitride is deposited using a low-pressure chemical vapor deposition (LPCVD) process. The silicon nitride and oxide are patterned on the backside of the wafer by dry SF₆ and buffered oxide etch (BOE), respectively. The diaphragms are not etched yet. Polysilicon is deposited using LPCVD on both front and back of the wafer on top of a 0.5- μm insulating oxide layer. The polysilicon on top of the wafer is doped with phosphorous to form the Wheatstone piezoresistor sensor bridge as well as heating resistors. The polysilicon on the back of the wafer will protect the patterned nitride until the backside etch is performed at the end of the process. A 1- μm low temperature oxide layer is deposited. The contact openings to poly and p+ silicon are etched out in a BOE solution. After the contacts are etched, a 1 μm Al layer is deposited, and, then patterned to make the electrical connections as well as to act as the bimetallic layer. An additional passivation oxide of 1 μm thickness is deposited on the front of the diaphragm in order to provide another layer of temperature isolation and prevent heat loss to the fluid under test. The front of the wafer is protected with Brewer Science's PROTEKTM. The diaphragms are formed by etching from the back of the wafers. The patterned silicon nitride is used as a protection layer during the silicon KOH-etch. The 1- μm -thick buried oxide of the SOI wafers serves as an etch-stop layer and as a thermal isolation layer on the back of the diaphragm.

A cross-section of the resulting structure is presented in Figure 2. The square membrane simplifies processing by using a well-established anisotropic KOH etch. Two types of heating schemes were used to determine the effect of the heating source to the response of the sensor. We use a p-type diffused silicon region, and, the polysilicon layer is the resistive heating elements.

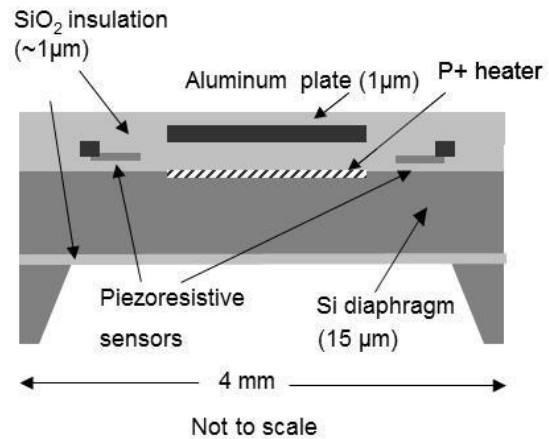


Figure 2. Cross-sectional view of the fabricated thermal actuator with a piezoresistive polysilicon bridge and an aluminium plate for enhanced bimetal actuation

The fabricated sensors were glued and wire bonded to a PCB board with an access hole drilled on its back. Both membrane surfaces are exposed. The vertical displacement was calculated based on the Wheatstone bridge output with a measured sensitivity of $1.35 \text{ mV}/\mu\text{m}$ when a 5 V supply is used [11]. An oscilloscope was used to monitor the bridge output in real-time through a LabView interface and software. The fast Fourier Transform is performed on the signal, statistical analysis is performed, distribution curves are fitted, etc. The natural frequency of vibration and the quality factor Q are calculated. This Q is calculated as the ratio of the peak frequency and the width at $\frac{1}{2}$ of the maximum amplitude.

4. VISCOSITY TESTING

The standard mineral oils and commercial motor oils, shown in Table 1, are used to perform viscosity measurements at room temperature. The viscosity and density reference standard oils are obtained from Koehler Instrument Company, Inc. An uncertainty between 0.07% and 0.17% is expected. The commercial motor oils were tested and their viscosity measured using a Brookfield DV-II+Pro cone-and-plate viscometer.

Table 1. Standard and commercial motor oils at $T=25^\circ\text{C}$

Oil	Kinematic Viscosity (25°C) mm^2/s or cSt	Density (25°C) g/mL
S3	4.035	0.8085
S6	8.792	0.8231
N10	17.01	0.8484
N35	65.07	0.8519
N100	238.7	0.8638
N350	824.2	0.8708
5W30	132.91	0.8860
10W40	211.49	0.8650
SAE60	644.20	0.8690

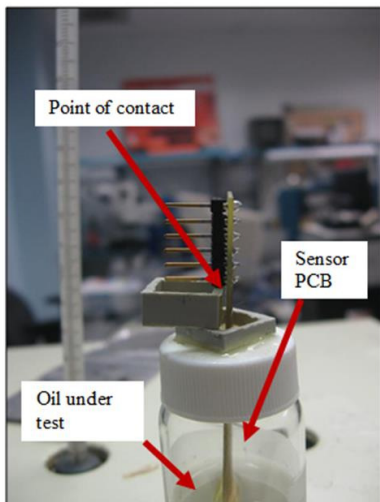


Figure 3. Side-view showing how the packaged sensor was positioned in the test fluid

The packaged sensors are fully submerged in the oil to be tested. Both surfaces of the diaphragm are in direct contact with the fluid. The PCB was suspended over the oil and held at a specified position as shown in Figure 3. The intent is to allow the sensor to vibrate freely without adding any external stress. External stress could be added if the PCB rested on the bottom or against the sides of the container. The devices always be positioned the same way in order to not to affect the natural vibration behavior.

Devices are tested in the standard oils with increasing viscosity. Then, they are tested in the commercial motor oils with viscosities falling within the range of the standard oils. Some cross-contamination happens in higher viscosity oils. This effect is found to be small. The same test conditions were used through the testing of devices. The typical settings were a Wheatstone Bridge bias of 5 V , a heating resistor bias at a frequency of 20 Hz with a voltage of -15 V for 30 microseconds and an amplifier gain of 50 as described in [12]. These conditions may be adjusted for each sensor.

Figure 4 shows the response of the sensor in the frequency domain measuring the fluid viscosity of the different standard and commercial samples presented in Table 1. The response indicates that amplitude, frequency, and quality factor decrease with increasing viscosity.

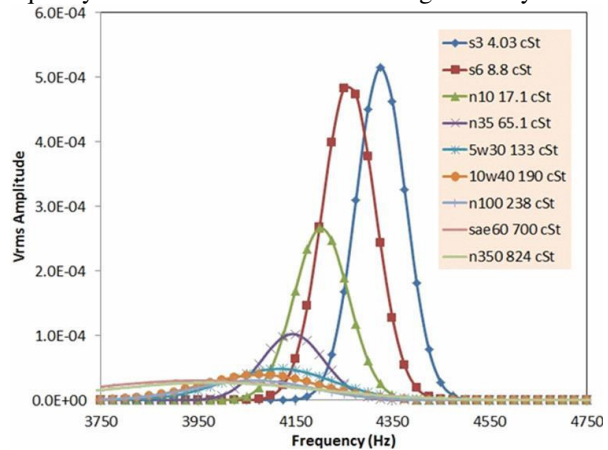


Figure 4. Typical frequency response of the sensor tested in oils of different viscosity at room temperature

Figure 5 shows the change in normalized frequency due to the change in viscosity for the MEMS sensors studied. The theoretical prediction using model [9] and [10] is shown for comparison. Trend lines are added to analyse the sensitivity. The error bars are added are a standard deviation. The results match prediction [10] for devices D11 and D12 which have $p+$ -diffused heaters as actuators. Devices 4D27 and 4D10 have poly heaters and have higher sensitivity than the theoretical predictions.

A similar analysis is performed for Q . Figure 6 shows the predicted values compared to the measured values for six sensors. The trend-lines help visualize the response and to confirm that they follow the same trend.

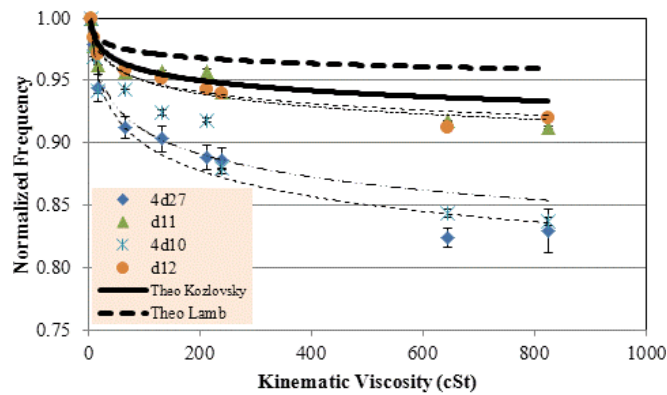


Figure 5. Normalized resonant frequency as a function of changes in viscosity compared to theoretical predictions for MEMS devices

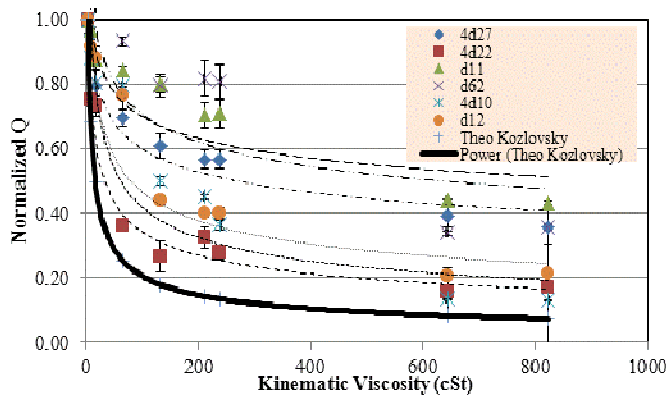


Figure 6. Normalized quality factor Q as a function of changes in viscosity compared to theoretical predictions for several devices

Despite a range of responses, the consistency is achieved. The quality factor is more sensitive to device losses due to the sensor defects, PCB positioning, packaging and other factors. These issues can be solved through technology refinements and quality control. The V_{rms} amplitude matches the trend better than the calculation for Q . The sensitivity improvement is shown in Figure 7. The theoretical prediction for Q [10] is plotted to use as an estimate. The frequency correlation to viscosity was shown to be the best indicator for the range of viscosities tested with lower error $\pm 5\%$, than that of quality factor which varies $\pm 20\%$.

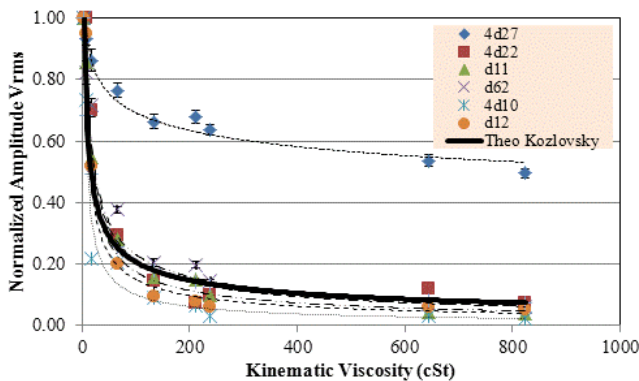


Figure 7. Normalized amplitude as a function of changes in viscosity compared to theoretical predictions for several devices.

5. CONCLUSIONS

We reported the fundamental, applied, experimental and technological solutions pertained to the measurements of viscosity of aqueous solutions. The CMOS-competitive MEMS devices are designed, tested, evaluated and characterized. Using the frequency and amplitude of the thermally induced vibrations of a silicon plate, and the plate damping due to the surrounding fluid, the viscosity is measured. Our results contribute to new technology developments, and, provide new practical solutions with a wide range of applications.

REFERENCES

- [1] M. M. Lara and C. Atkinson, "Theoretical model on the interaction of a vibrating beam and the surrounding viscous fluid with applications to density and viscosity sensors," *Proc. IEEE Sensors*, pp. 828-831, 2004.
- [2] N. Belmiloud, I. Dufour, L. Nicu, A. Colin and J. Pistre, "Vibrating Microcantilever used as a viscometer and microrheometer," *IEEE Sensors 2006, EXCO*, Daegu, Korea, pp. 753-756, 2006.
- [3] C. Harrison, A. Fornari, C. Hua, S. Ryu, A.R. Goodwin, K. Hsu, F. Marty and B. Mercier, "A microfluidic MEMS sensor for the measurement of density and viscosity at high pressure," *Proc. SPIE*, vol. 6465, 2007.
- [4] A. Ramkumar, X. Chen and A. Lal, "Silicon ultrasonic horn driven microprobe viscometer," *Proc. IEEE Ultrasonics Symposium*, pp. 1449-1452, 2006.
- [5] C. Ayela and L. Nicu, "Micromachined piezoelectric membranes with high nominal quality factors in Newtonian liquid media: a Lamb's model validation at the microscale," *Sensors and Actuators B*, vol. 123, pp. 860-868, 2007.
- [6] I. Goubaidouline, J. Reuber, F. Merz and D. Johannsmann, "Simultaneous determination of density and viscosity of liquids based on quartz-crystal resonators covered with nanoporous alumina," *J. Applied Physics*, vol. 98, pp. 0143051-0143054, 2005.
- [7] B. A. Martin, "Viscosity and density sensing with ultrasonic plate waves," *Sensors and Actuators A: Physical*, vol. 22, pp. 704-708, 1990.
- [8] R. D. Blevins, *Formulas for Natural Frequency and Mode Shape*, New York, Van Nostrand Reinhold Company, 1979.
- [9] H. Lamb, "On the vibrations of an elastic plate in contact with water," *Proc. Royal Society of London. Series A, Containing Papers of a Mathematical and Physical Character*, vol. 98, p. 205-216, 1920.
- [10] Y. Kozlovsky, "Vibration of plates in contact with viscous fluid: Extension of Lamb's model," *J. Sound and Vibration*, vol. 326, pp. 332-339, 2009.
- [11] I. Puchades and L. Fuller, "Design and evaluation of a MEMS bimetallic thermal actuator for viscosity measurements," *University/Government/Industry Micro-Nano Symposium, UGIM*, pp. 93-96, 2008.
- [12] I. Puchades and L. Fuller, "A thermally actuated micro-electromechanical device for measuring viscosity," *J. Micro-electromechanical Systems*, vol. 20, no. 3, pp. 601-608, 2011.